Cyanomethylene Formation from the Reaction of Excited Nitrogen Atoms with Acetylene: A Crossed Beam and ab Initio Study

N. Balucani,[§] M. Alagia,[#,§] L. Cartechini,[§] P. Casavecchia,*[,§] G. G. Volpi,[§] K. Sato,[†,||] T. Takayanagi,[⊥] and Y. Kurosaki[‡,⊥]

Contribution from the Dipartimento di Chimica, Università di Perugia, 06123 Perugia, Italy, Department of Applied Physics, Tokyo Institute of Technology, Ookayama, Meguro-ku, Tokyo 152-8551, Japan, and Advanced Science Research Center, Japan Atomic Energy Research Institute, Tokai-mura, Naka-gun, Ibaraki 319-1195, Japan

Received September 23, 1999

Abstract: The reaction of excited nitrogen atoms, $N(^2D)$, with the simplest alkyne, C_2H_2, was investigated for the first time under single-collision conditions in crossed beam experiments with mass spectrometric detection. The experimental results combined with electronic structure calculations and RRKM predictions allow us to identify cyanomethylene (HCCN) as the main primary reaction product and to establish its formation dynamics. The identification of the N/H exchange channel suggests that the title reaction is a good candidate to explain formation of nitriles in the upper atmosphere of Titan.

Introduction

Chemical reactions of nitrogen atoms are significant in a variety of systems, from atmospheric to interstellar chemistry and from plasma to combustion chemistry. The investigation of N atom reactions has always represented a challenge to chemists who resorted to "active nitrogen" (a mixture of ground, $N(^4S)$, and excited-state atomic, $N(^2D)$ and $N(^2P)$, and molecular, $N_2(^3\Sigma_u^+)$, nitrogen) to gain information on the kinetics.[1] Those data were mostly interpreted on the assumption that the only reactive species was the ground-state atom, $N(^4S)$, though the presence of the excited states, $N(^2D)/N(^2P)$, and also of excited molecular nitrogen, $N_2(^3\Sigma_u^+)$, made it difficult to assess the role of each species. Nowadays, thanks to recent and more reliable kinetic data, we know that $N(^4S)$ is rather unreactive when the partner is a closed shell molecule,[2−4] while $N(^2D)$ (the first electronic excited state lying 230.5 kJ mol^{-1} above the ground state) is much more reactive.[5] Yet, despite recent efforts in measuring the rate constants of N atom reactions, the reaction mechanisms have only been speculated and the primary reaction products not directly identified.

A deeper understanding of the reaction mechanism requires investigation at the molecular level, where it is possible to observe the consequences of a single reactive event. Unfortunately, investigation of N atom reactions at the microscopic level eluded for a long time the experimental techniques in the field of reaction dynamics. For instance, the application of the crossed molecular beam (CMB) technique was hampered by the difficulty of generating supersonic beams of N atoms of sufficient intensity to carry out angular and velocity distribution measurements of the reaction products.[6] Only in the last two years have the nascent internal distributions of NH formed from $N(^2D)$ reactions with simple molecules been determined by laser-induced fluorescence,[7] while in our laboratory we have succeeded in generating supersonic beams of nitrogen atoms of sufficient intensity to be employed in reactive scattering experiments and have recently studied the reaction $N(^2D) + H_2 \rightarrow NH + H$ using the CMB technique with mass spectrometric detection.[8] We recall that the CMB technique is particularly suitable for investigating reactions giving polyatomic products which are not a priori predictable and/or whose spectroscopic properties are unknown.[9]

Here, we report for the first time on the dynamics of a reaction of nitrogen atoms with an unsaturated hydrocarbon by com-

* Address correspondence to this author.
[§] Università di Perugia.
[#] Present address: INFM, Sincrotrone Elettra, 34012 Trieste, Italy.
[†] Present address: Division of Atmospheric Environment, The National Institute for Environmental Studies, 16-2 Onogawa, Tsukuba, Ibaraki, 305-0053, Japan.
[||] Tokyo Institute of Technology.
[⊥] Japan Atomic Energy Research Institute.
[‡] Present address: Advanced Photon Research Center, Japan Atomic Energy Research Institute, Umemidai, Kizu-cho, Soraku-gun, Kyoto 619-0215, Japan.

(1) Wright, A. N.; Winkler, C. A. *Active Nitrogen*; Academic Press: New York and London, 1968.
(2) (a) Black, G.; Slanger, T. G.; St. John, G. A.; Young, R. A. *J. Phys. Chem.* **1969**, *51*, 116−121. (b) Iannuzzi, M. P.; Kaufman, F. *J. Chem. Phys.* **1980**, *73*, 4701−4702. (c) Fell, B.; Rivas, I. V.; McFadden, D. L. *J. Phys. Chem.* **1981**, *85*, 224−228. (d) Donovan, R. J.; Husain, D. *Chem. Rev.* **1970**, *70*, 489−516.
(3) Michael, J. V. *Chem. Phys. Lett.* **1980**, *76*, 129−131.
(4) Umemoto, H.; Nakagawa, S.; Tsunashima, S.; Sato, S. *Bull. Chem. Soc. Jpn.* **1986**, *59*, 1449−1454.
(5) (a) Umemoto, H.; Sugiyama, K.; Tsunashima, S.; Sato, S. *Bull. Chem. Soc. Jpn.* **1985**, *58*, 3076−3081. (b) Umemoto, H.; Hachiya, N.; Matsunaga, E.; Suda, A.; Kawasaki, M. *Chem. Phys. Lett.* **1998**, *296*, 203−207.
(6) For the only reported attempts, see: (a) Love, R. L.; Herrmann, J. M.; Bickes, R. W.; Bernstein, R. B. *J. Am. Chem. Soc.* **1977**, *99*, 8316−8317. (b) Porter, R. A. R.; Brown, G. R.; Grosser, A. E. *Chem. Phys. Lett.* **1979**, *61*, 313−314.
(7) (a) Umemoto, H.; Asai, T.; Kimura, Y. *J. Chem. Phys.* **1997**, *106*, 4985−4991. (b) Umemoto, H.; Nakae, T.; Hashimoto, H.; Kongo, K.; Kawasaki, M. *J. Chem. Phys.* **1998**, *109*, 5844−5848. (c) Umemoto, H.; Asai, T.; Hashimoto, H.; Nakae, T. *J. Phys. Chem. A* **1999**, *103*, 700−704.
(8) (a) Alagia, M.; Balucani, N.; Cartechini, L.; Casavecchia, P.; Volpi, G. G.; Pederson, L. A.; Schatz, G. C.; Harding, L. B.; Hollebeek, T.; Ho, T.-S.; Rabitz, H. *J. Chem. Phys.* **1999**, *110*, 8857−8860. (b) Casavecchia, P.; Balucani, N.; Alagia, M.; Cartechini, L.; Volpi, G. G. *Acc. Chem. Res.* **1999**, *32*, 503−511.
(9) Lee, Y. T. In *Atomic and Molecular Beam Methods*; Scoles, G., Ed.; Oxford University Press: New York, 1987; Vol. 1, pp 553−568.

10.1021/ja993448c CCC: $19.00
Published on Web 04/18/2000

bining crossed molecular beam experiments and ab initio molecular orbital calculations. The reaction in question is $N(^2D) + C_2H_2(^1\Sigma_g^+)$: our study identifies HCCN (cyanomethylene) as the main reaction product and characterizes its formation dynamics.

Early kinetic work[10] on the reactions of "active nitrogen" with acetylene suggested that the main products are HCCN + H; however, the electronic state of the N atom and the reaction products were not identified. More recent studies[3,4] reported the rate constant for the reaction $N(^4S) + C_2H_2$ to be immeasurably low ($k \sim 10^{-16}$ cm^3 molecule^{-1} s^{-1}) at room temperature, while that of $N(^2D)$ has been determined[2] to be 1.1×10^{-10} cm^3 molecule^{-1} s^{-1} and, very recently,[11] 6.7×10^{-11} cm^3 molecule^{-1} s^{-1}. The rate constant for the reaction $N(^2P) + C_2H_2$ has been determined[2c,11] to be 2.3×10^{-11} cm^3 molecule^{-1} s^{-1}, about a factor of 3 (5) smaller than that of $N(^2D)$ from ref 11 (ref 2c). A lower reactivity of $N(^2P)$ (lying 343.5 kJ mol^{-1} above the ground state) with respect to $N(^2D)$ is not surprising considering that $N(^2P) + C_2H_2$ does not correlate adiabatically with ground-state products.[2d] On this basis, earlier work[5a] suggested that the main deactivation pathway of $N(^2P)$ is physical quenching to $N(^2D)$, followed eventually by reaction.

Within the wider scientific community the relevance of the reactions of $N(^2D)$ with C_2H_2 and other hydrocarbons is mainly related to its alleged role in the chemistry of Saturn's moon Titan as the first step in the formation of molecules containing a C−N bond.[12] Titan is a satellite with massive atmosphere reminiscent of the primordial atmosphere of the Earth and for this reason has attracted considerable attention during the past two decades. Extensive photochemical modelings of its atmosphere have been worked out, which comprise complex chemical reaction networks. The pre-Voyager models, restricted to hydrocarbons, turned out to be unrealistic when the Voyager missions provided evidence that N_2 is the principal constituent of Titan's atmosphere, followed by CH_4, H_2, C_2H_2, C_2H_4, C_2H_6, CH_3C_2H, C_3H_8, HCN, HC_3N, C_2N_2, C_4N_2, etc. Therefore, it is necessary to also consider reactions between active forms of nitrogen and hydrocarbons to understand the chemistry of Titan's atmosphere and explain the presence of CN-containing molecules. The first detailed photochemical model after the Voyager mission was developed by Yung et al.[13] and updated by Yung.[12a] These studies followed earlier work by Strobel,[14] Allen et al.,[15] and Strobel.[16] Improved photochemical models, which draw on the previous ones, have been recently reported.[17,18a,b] It is clear, from the very complete set of chemical reactions included in these models, that the presence of N_2 allows the formation of nitriles from nitrogen atoms and ions in the thermosphere, mesosphere, and upper stratosphere. In particular, the formation of nitrile compounds in Titan's reducing atmosphere is initiated by the dissociation of N_2: electron impact, extreme-ultra-violet photolysis ($\lambda < 80$ nm), galactic cosmic ray absorption, N_2^+ dissociative recombination, all lead to formation of ground-state $N(^4S)$ and electronically excited $N(^2D)$ atoms.[18a] The net production of N atoms from photolysis and galactic cosmic ray impact of N_2 is 1.1×10^9 cm^{-2} s^{-1}, while the value from magnetospheric electrons is 7×10^7 cm^{-2} s^{-1};[18a] in the model, most of the N atoms liberated from the N_2 destruction end up in compounds, with fluxes of CH_2NH and C_2H_3CN larger than 9×10^8 cm^{-2} s^{-1}. Since collisional deactivation of metastable $N(^2D)$ (radiative lifetime 17−40 h) to $N(^4S)$ by N_2 is a slow process ($k_{298} \sim 1.6 \times 10^{-14}$ cm^3 molecule^{-1} s^{-1}),[18a,19] the main fate of $N(^2D)$ above 800 km is, on the basis of the relative reaction rates and abundances,[18a] chemical reaction with other constituents of Titan's atmosphere, such as H_2, CH_4, C_2H_2, C_2H_4, etc. Although physical quenching becomes more important with decreasing altitudes due to the decreasing concentrations of the above species, a significant fraction of $N(^2D)$ can still undergo chemical reactions down to the lower stratosphere. In some respect, $N(^2D)$ is supposed to play in Titan's atmosphere a role similar to that played by $O(^1D)$ in the Earth's atmosphere.

To explain the formation of nitrile compounds, the reaction of $N(^4S)$ with CH_3 radicals was initially thought[13] to be the primary source of formation of HCN and, hence, of nitrile compounds through the reaction CN + HCN → C_2N_2 + H. Later, however, cyanomethylene (HCCN) was proposed by Yung[12a] as an important intermediate produced in the atmosphere of Titan that leads to the formation of nitriles such as cyanogen, C_2N_2, and dicyanogen (dicyanoacetylene), C_4N_2, and could explain some of the Voyager observations (mixing ratios and vertical profiles). Specifically, the reaction between C_2H_2 (one of the most abundant hydrocarbons) and $N(^2D)$ was proposed as the source of HCCN, provided the rate coefficient is 1×10^{-11} cm^3 molecule^{-1} s^{-1}. The most likely fate of HCCN would then be reaction with N atoms to give C_2N_2 + H or disproportionation to $C_4N_2 + H_2$, two strongly exoergic processes. A call was made by Yung for experimental investigations of the reaction $N(^2D) + C_2H_2$ which could support this hypothesis. The most recent photochemical model (from 40 to 1432 km)[18a,b] for calculating the vertical distribution of Titan's neutral atmosphere compounds still refers to this hypothesis to account for the production of cyanogen and dicyanogen. Very recently, C_4N_2 (dicyanoacetylene) was for the first time observed in laboratory simulations of Titan's atmosphere starting from discharges in N_2-CH_4 mixtures.[20a] This detection confirms that formation of C_4N_2 in Titan's environment could occur, probably by the way of the reaction $C_2H_2 + N(^2D)$ → HCCN + H followed by 2HCCN → $C_4N_2 + H_2$.[20b]

On the theoretical side, ab initio electronic structure calculations[11,21] have recently been carried out by some of the present authors for understanding the mechanisms and dynamics of the $N(^2D) + C_2H_2$ reaction. It has been found theoretically that the addition of the $N(^2D)$ to the triple bond to initially form a three-membered intermediate radical is the lowest reaction pathway.[11] Possible final products have also been predicted. More recently, variational transition-state theory calculations have been done for the $N(^2D) + C_2H_2$ reaction using the results of ab initio calculations and it has been suggested that nonadiabatic transitions play a role in this reaction.[21]

(10) (a) Safrany, D. R. *Prog. React. Kinet.* **1971**, *6*, 1−49. (b) Safrany, D. R.; Jaster, W. *J. Phys. Chem.* **1968**, *72*, 3305−3318.
(11) Takayanagi, T.; Kurosaki, Y.; Misawa, K.; Sugiura, M.; Kobayashi, Y.; Sato, K.; Tsunashima, S. *J. Phys. Chem. A* **1998**, *102*, 6251−6258.
(12) (a) Yung, Y. L. *Icarus* **1987**, *72*, 468−472. (b) Toublanc, D.; Parisot, J. P.; Brillet, J.; Gautier, D.; Raulin, F.; McKay, C. P. *Icarus* **1995**, *113*, 2−26.
(13) Yung, Y. L.; Allen, M.; Pinto, J. P. *Astrophys. J. Suppl. Ser.* **1984**, *55*, 465−506.
(14) Strobel, D. F. *Icarus* **1974**, *21*, 466.
(15) Allen, M.; Pinto, J. P.; Yung, Y. L. *Astrophys. J.* **1980**, *242*, L125.
(16) Strobel, D. F. *Planet. Space Sci.* **1982**, *30*, 839.
(17) Toublanc, D.; Parisot, J. P.; Brillet, J.; Gautier, D.; Raulin, F.; McKay, C. P. *Icarus* **1995**, *113*, 2−26.
(18) (a) Lara, L. M.; Lellouch, E.; Lopez-Moreno, J. J.; Rodrigo, R. *J. Geophys. Res.* **1996**, *101*, 23261−23283. (b) Lunine, J. I.; Yung, Y. L.; Lorenz, R. D. *Planet. Space Sci.* **1999**, *47*, 1291−1303.
(19) Donovan, R. J.; Husain, D. *Chem. Rev.* **1970**, *70*, 489−516.
(20) (a) Coll, P.; Coscia, D.; Smith, N.; Gazeau, M.-C.; Ramírez, S. I.; Cernogora, G.; Israël, G.; Raulin. F. *Planet. Space Sci.* **1999**, *47*, 1331−1340. (b) Coll, P.; Guillemin, J.-C.; Gazeau, M.-C.; Raulin. F. *Planet. Space Sci.* **1999**, *47*, 1433−1440.
(21) Takayanagi, T.; Kurosaki, Y.; Yokoyama, K.; Sato, K.; Tsunashima, S. *Chem. Phys. Lett.* **1999**, *312*, 503−510.

The present investigation exploits the novel capability of generating intense supersonic beams of N(^{2}D) atoms, which has opened up the possibility of studying the reactive scattering of atomic nitrogen under single collision conditions. Direct identification of the N/H exchange channel has allowed us to assess the primary product and, with the support of further theoretical work, its dynamics of formation, hence, to assess its potential relevance to Titan's atmospheric chemistry.

Experiment Section

We performed scattering experiments at two different collision energies (E_c = 13.0 and 39.7 kJ mol^{-1}) using a universal crossed molecular beam apparatus that has been described elsewhere.[22] Briefly, two well-collimated, in angle and velocity, supersonic beams of the reagents are crossed at 90° in a large scattering chamber maintained in the 10^{-7}-mbar range. The angular and velocity distributions of the products are measured by a rotatable electron impact quadrupole mass spectrometer detector, contained in an ultrahigh-vacuum (10^{-11} mbar) chamber.

Continuous supersonic beams of N atoms are generated from a high-pressure, high-power radio frequency (rf) discharge beam source,[8,22] similar in design to that described by Sibener et al.[23] for oxygen atom beam production, and which has been successfully used in our laboratory for O(^{3}P,^{1}D) and Cl beams, OH beams,[8,22,24] and, recently, also for C(^{3}P,^{1}D) and CN beams.[24a] Two N beams with different translational energies were produced to vary the relative collision energy of the experiment. By discharging 375 mbar of a 2.5% N_2 in helium gas mixture through a 0.25 mm diameter quartz nozzle at 300 W of rf power, a beam with peak velocity of 2888 m s^{-1} and speed ratio of 7.6 was obtained. By discharging 300 mbar of a 2.5% N_2 in neon gas mixture through the same quartz nozzle at 300 W of rf power, a beam with a peak velocity of 1519 m s^{-1} and a speed ratio of 5.9 was produced. The N beams were skimmed by a 1 mm diameter boron nitride skimmer and further defined by a rectangular slit to an angular divergence of 2.3°. Using the fast and slow beams of nitrogen atoms, relative collision energies, E_c, of 39.7and 13.0 kJ mol^{-1}, respectively, were obtained. Due to the very efficient coupling of the rf power to the plasma, this procedure leads to more than 60% dissociation of molecular N_2 and to a distribution of electronic states of atomic nitrogen. The latter has been characterized by Stern−Gerlach magnetic analysis:[24b] 72% of the N atoms are found in the ground ^{4}S state, and 21% and 7% in the first excited ^{2}D and ^{2}P states, respectively. As we will see below, only N(^{2}D) is contributing to the reactive scattering signal.

A supersonic beam of acetylene was generated by expanding 290 mbar of C_2H_2 through a 0.1 mm diameter stainless steel nozzle kept at room temperature. A CO_2/acetone slush trap was used on the C_2H_2 gas line to trap acetone impurities. An electroformed nickel skimmer defined the beam to an angular divergence of 5.7°. The peak velocity was 821 m s^{-1} and the speed ratio was 6.6. Under this expansion conditions C_2H_2 clustering was negligible. Because of the significant cooling during supersonic expansion, the acetylene molecules in the beam are expected to be in the lowest rotational states of essentially the ground vibrational level, and therefore the internal energy of the molecular reactant contributes negligibly to the total available energy.

Angular distributions of the reaction product (C_2HN, see below) were obtained by taking at least five scans of 50 s counts at each angle. The C_2H_2 beam was modulated at 160 Hz by a tuning-fork chopper for background subtraction. Velocity analysis of the beams was carried out by conventional "single-shot" time-of-flight (TOF) techniques, using a high-speed multichannel scaler and a CAMAC data acquisition system controlled by a personal computer. Velocity distributions of products were obtained at seven different angles only at the highest E_c = 39.7 kJ mol^{-1} using the cross-correlation TOF technique[25] with four 127-bit pseudorandom sequences. High-time resolution was achieved by spinning the TOF disk, located at the entrance of the detector, at 393.7 Hz corresponding to a dwell time of 5 μs/channel. The flight length was 24.5 cm. Counting times varied from 30 to 60 min depending upon signal intensity.

Ab Initio Electronic Structure and Rice−Ramsperger−Kassel−Marcus (RRKM) Calculations

Ab initio electronic structure calculations were performed to predict the relative energies of all local minima, transition states, and exothermicities of the possible channels for the N(^{2}D) + C_2H_2($^1\Sigma_g^+$) reaction, with particular focus on the possible isomer products arising from the N/H exchange channel. The computational method is almost the same as described in ref 11 except that an additional three HCCN isomers (singlet linear-HCCN and singlet and triplet cyclic-HC(N)C) are included as final products. The relative energies were calculated by the spin-projected fourth-order Møller−Plesset theory with the correlation-consistent polarized valence triple-ζ (cc-pVTZ) basis set of Dunning.[26] Geometry optimizations for all stationary points were carried out at the second-order fourth-order Møller−Plesset level of theory with the cc-pVTZ basis set. Zero-point energy corrections were carried out using vibrational frequencies calculated at the same level of theory. All the calculations were performed with the GAUSSIAN 94 program package.[27] With the level of theory employed, the errors in the energies are smaller than 30 kJ mol^{-1}. The lowest doublet potential energy surface has been considered, but the transition state structure and the barrier height of the ground-state N(^{4}S) + C_2H_2($^1\Sigma_g^+$) reaction have been computed as well.

Since the reaction mechanisms are somewhat complicated, it may be difficult to predict main products only from the energy diagram. Therefore, we have perfomed RRKM calculations to estimate branching fractions of products under collision-free conditions. The unimolecular rate constants for isomerizations and dissociations were calculated by standard RRKM theory with the Whitten−Ravinovich approximation[28] by using the vibrational frequencies obtained from the ab initio calculations. To estimate the product branching fractions, the kinetic equations were numerically solved. Details of the calculations are also described in ref 29.

Results

Laboratory Product Angular Distributions and Time-of-Flight Spectra. Reaction products were detected only at a mass-to-charge ratio of *m*/*e* 39 (C_2HN^+) and 38 (C_2N^+). The laboratory angular distributions at *m*/*e* 39 and 38 at E_c = 39.7 kJ mol^{-1} are shown in Figure 1: they appear to be superimposable which unambiguously indicates that C_2HN fragments partly to C_2N^+ in the electron impact ionizer. This dismisses the occurrence of the strongly exoergic CCN($^2\Pi$) + H_2($^1\Sigma_g^+$) pathway ($\Delta H°_0 \approx -210$ kJ mol^{-1}), which is not surprising considering that CCN formation would imply a four-center molecular hydrogen elimination, a kind of process that is usually characterized by a very high exit potential barrier. Because of the higher S/N ratio (S/N = 56 versus S/N = 21 with 50 s

(22) Alagia, M.; Balucani, N.; Casavecchia, P.; Stranges, D.; Volpi, G. G. *J. Chem. Soc., Faraday Trans.* **1995**, *91*, 575−596.
(23) Sibener, S. J.; Buss, R. J.; Ng, C. Y.: Lee, Y. T. *Rev. Sci. Instrum.* **1980**, *51*, 167−182.
(24) (a) Casavecchia, P. *Rep. Prog. Phys.* **2000**, *63*, 355−414. (b) Alagia, M.; Aquilanti, V.; Ascenzi, D.; Balucani, N.; Cappelletti, D.; Cartechini, L.; Casavecchia, P.; Pirani, F.; Sanchini, G.; Volpi, G. G. *Isr. J. Chem.* **1997**, *37*, 329−342.
(25) Skold, K. *Nucl. Instrum. Methods* **1968**, *63*, 114.
(26) Dunning, T. H., Jr. *J. Chem. Phys.* **1989**, *90*, 1007−1023.
(27) Frisch, M. J.; Trucks, G. W.; Schlegel, H. B.; Gill, P. M. W.; Johnson, B. G.; Robb, M. A.; Cheeseman, J. R.; Keith, T.; Petersson, G. A.; Montgomery, J. A.; Raghavachari, K.; Al-Laham, M. A.; Zakrzewski, V. G.; Ortiz, J. V.; Foresman, J. B.; Cioslowski, J.; Stefanov, B. B.; Nanayakkara, A.; Challacombe, M. C.; Peng, Y.; Ayala, P. Y.; Chen, W.; Wong, M. W.; Andres, J. L.; Replogle, E. S.; Gomperts, R.; Martin, R. L.; Fox, D. J.; Binkley, J. S.; Defrees, D. J.; Baker, J.; Stewart, J. P.; Head-Gordon, M.; Gonzalez, C.; Pople, J. A. Gaussian 94; Gaussian, Inc.: Pittsburgh, PA, 1995.
(28) Holbrook, A.; Pilling, M. J.; Robertson, S. H. *Unimolecular Reactions*; John Wiley: Chichester, 1996.
(29) Takayanagi, T.; Kurosaki, Y.; Sato, K.; Tsunashima, S. *J. Phys. Chem. A* **1998**, *102*, 10391−10398.

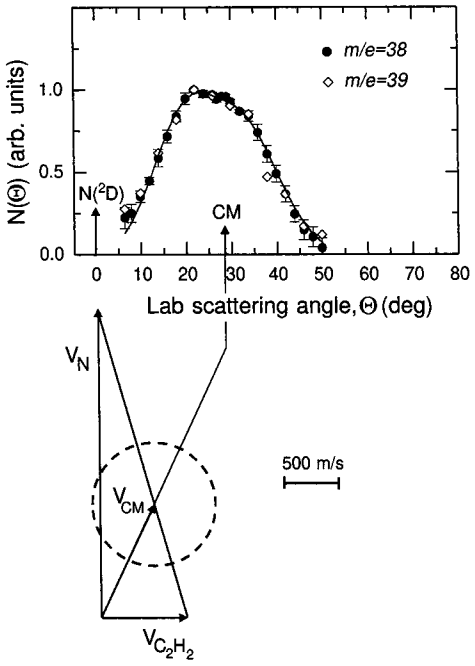

Figure 1. The C_2HN product laboratory angular distribution (detected at *m*/*e* 38 (dots) and *m*/*e* 39 (diamonds)) from the reaction $N(^2D) + C_2H_2(^1\Sigma_g^+)$ at a relative collision energy $E_c = 39.7$ kJ mol^{-1}, together with the canonical velocity vector ("Newton") diagram of the experiment. The solid line represents the angular distribution obtained from the best-fit CM angular and translational energy distributions. The dashed circle in the Newton diagram delimits the maximum speed that the linear HCCN product can attain if all the avalaible energy is channeld into product translational energy.

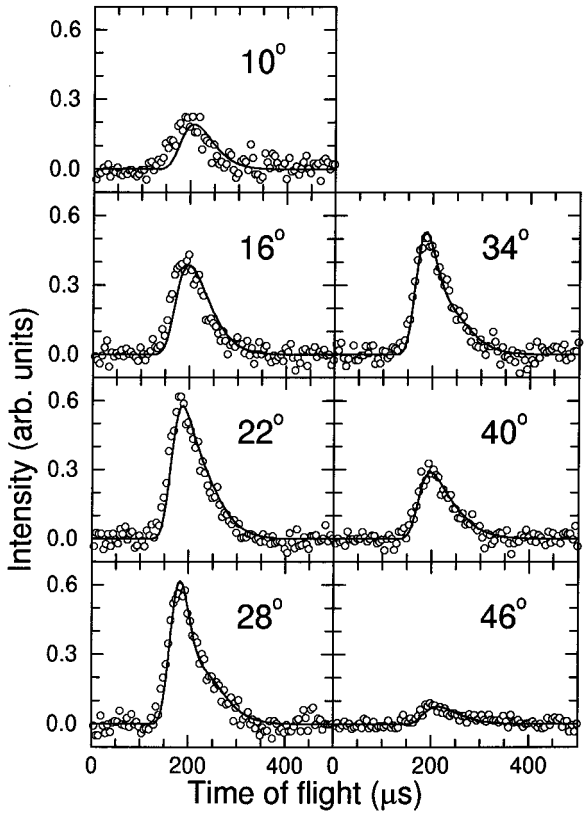

Figure 2. The C_2HN product (detected at *m*/*e* 38) time-of-flight distributions at the indicated laboratory angles from the reaction $N(^2D) + C_2H_2(^1\Sigma_g^+)$ at a relative collision energy $E_c = 39.7$ kJ mol^{-1}. The time scale is absolute, the ion flight time and electronic offsets having been taken into account. The distributions are normalized to the relative intensities at each angle. Solid lines: Calculation with best-fit CM translational energy and angular distributions of Figure 4.

counting time), all other measurements were carried out at *m*/*e* 38. The time-of-flight (TOF) distributions at seven selected angles for $E_c = 39.7$ kJ mol^{-1} are shown in Figure 2; these distributions have been normalized to the relative intensities at each angle. No radiative association to C_2H_2N was detected, indicating that under single-collision conditions the formed adducts fragment because of their high energy content. The product angular distribution at $E_c = 13.0$ kJ mol^{-1} is reported in Figure 3; the error bars here are considerably larger than those at the higher E_c because of the considerably lower reactive scattering signal with respect to the high E_c experiment, and no TOF distributions could be measured. This is due to the lower intensity (by about a factor 5) of the neon-seeded N beam with respect to the He-seeded N beam and of a reaction cross section that decreases with decreasing collision energy. Observation of product at $E_c = 13.0$ kJ mol^{-1} indicates that the calculated barrier to reaction of 12 kJ mol^{-1} (see below) is likely to be too high, corroborating the indication emerged from rate constant measurements[11] which find an activation energy for reaction of only 2 kJ mol^{-1}. The solid lines in Figures 1−3 show the calculated best-fit (see below).

The laboratory angular and velocity distribution results indicate unambiguously that the *m*/*e* 39 product (C_2HN) is a main primary reaction product. The lab angular distributions exhibit intensity on both sides of the center-of-mass angle, and this already indicates that the reaction is not direct; its width reflects the amount of energy channelled into product recoil energy.

Center-of-Mass Angular and Translational Energy Distributions. To obtain quantitative information on the reaction dynamics one has to move from the laboratory system of coordinates to the center-of-mass (CM) frame of reference[9,22] and analyze the CM product flux distribution $I_{CM}(\theta,E'_T)$, i.e., the double differential cross section. This is assumed to be separable into the product of a translational energy and an angular part, $I_{CM}(\theta,E'_T) = T(\theta)P(E'_T)$. The product angular, $T(\theta)$, and translational energy, $P(E'_T)$, distributions in the CM frame are derived by a forward convolution fit of the product laboratory angular and TOF distributions. In the analysis procedure,[22] the CM angular and translational energy distributions are input as trial functions; the corresponding laboratory angular and TOF distributions are then calculated and compared to the experimental data. The experimental resolution broadening, due to the TOF disk and detector slit sizes, disk velocity and ionizer length, and spread in beam velocities and angular divergences, is taken into account. The original trial functions are adjusted and the process repeated until a satisfactory fit is obtained to both the TOF spectra and the angular distributions. The best-fit calculations to the experimental angular and TOF distributions are shown as solid lines in the Figures 1−3. Figure 4 shows the resultant CM angular distributions, $T(\theta)$, and translational energy distributions, $P(E'_T)$, for the two E_c. The final result of the data fitting analysis is a CM contour map of product flux as a function of angle and product recoil energy.[9,30] After a straightforward transformation to convert the flux distribution from an energy space to a velocity space, the CM contour maps $I_{CM}(\theta,u)$, where u is the CM product velocity, are represented in polar form in Figure 5. The transformation of the CM flux $I_{CM}(\theta,u)$ to laboratory number density $N(\Theta)$ is given by $N(\Theta) = (v/u^2)I_{CM}(\theta,u)$. The effect of the Jacobian v/u^2 for the

(30) Levine, R. D.; Bernstein, R. B. *Molecular Reaction Dynamics and Chemical Reactivity*; Oxford University Press: New York, 1987.

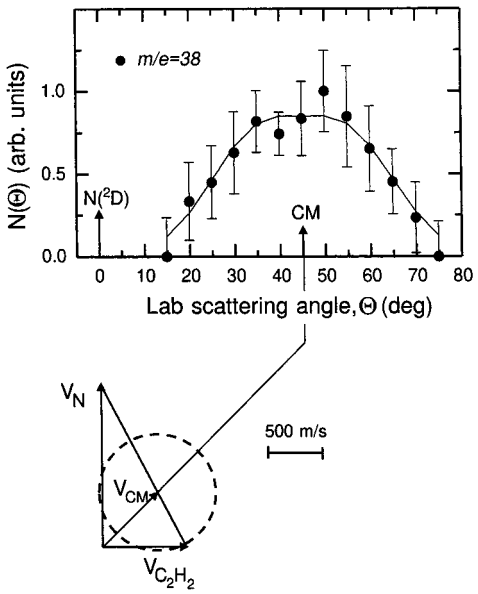

Figure 3. The C_2HN product laboratory angular distribution (detected at *m/e* 38) from the reaction $N(^2D) + C_2H_2(^1\Sigma_g^+)$ at $E_c = 13.0$ kJ mol^{-1}, together with the canonical velocity vector ("Newton") diagram of the experiment. The solid line represents the angular distribution obtained from the best-fit CM angular and translational energy distributions. The dashed circle in the Newton diagram delimits the maximum speed that the linear HCCN product can attain if all the avalaible energy is channeld into product translational energy.

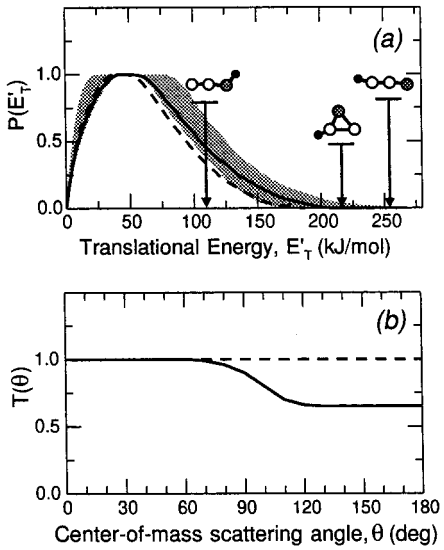

Figure 4. Best-fit CM product translational energy (a) and angular (b) distributions. Solid lines: CM functions at E_c=39.7 kJ mol^{-1}. Dashed lines: CM functions at $E_c = 13.0$ kJ mol^{-1}. In panel a the shaded area delimits the error bars of the experimental determination for $E_c = 39.7$ kJ mol^{-1} and the arrows delimit the maximum energy ($E_c - \Delta H°_{reaction}$) reachable by the three different isomers corresponding to the general formula C_2HN.

coordinate transformation results in a strong enhancement of the low-energy products. In fact, while the product flux actually peaks fairly well removed from the CM position on the relative velocity axis (see Figure 5), the measured lab angular distributions, $N(\Theta)$, do not show pronounced dips around the lab CM angle (see Figures 1 and 3).

The CM product angular distribution contains information about the micromechanism of the reaction, i.e., its shape tells us whether the reaction is direct or proceeds via the formation of a long-lived complex intermediate,[30,31] while the product

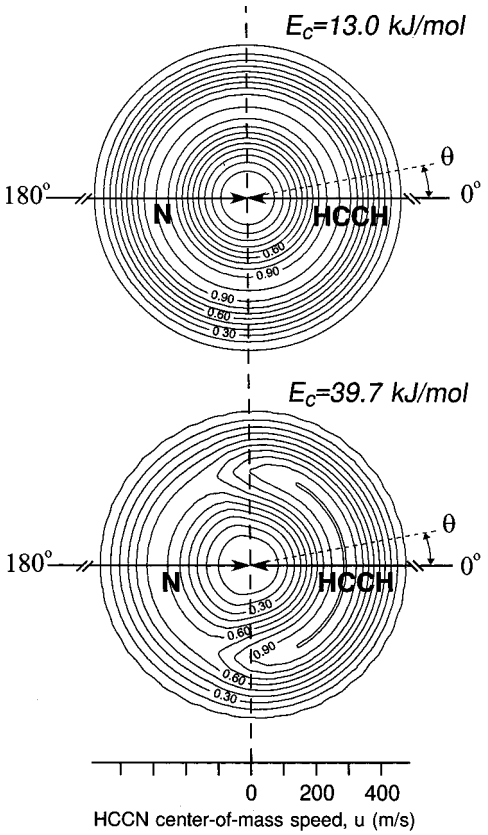

Figure 5. CM polar flux (velocity-angle) contour maps of the HCCN product at $E_c = 13.0$ kJ mol^{-1} (top) and $E_c = 39.7$ kJ mol^{-1} (bottom). $\theta = 0°$ indicates the forward direction with respect to the incoming N beam; the shift from backward−forward symmetric scattering toward forward scattering of the HCCN product with increasing E_c is clearly visible.

translational energy distribution provides a measure of the product energy partitioning between internal and translational degrees of freedom; their features are ultimately determined by the characteristics of the potential energy surface governing the reaction.

The best-fit CM angular distributions (Figure 4b) show intensity in the whole angular range and are indicative of the formation of a bound intermediate during the reaction and of a significant product rotational excitation (see Discussion). The extent of the energy release, revealed by the shape of the $P(E'_T)$ (Figure 4a), gives us a criterion (through the energy conservation rule[30]) to establish which products of general formula C_2HN are possible. The $P(E'_T)$ functions peak at about 38 and 42 kJ mol^{-1}, and correspond to an average fraction of energy released in translation, defined as $\langle E_T \rangle = \sum P(E'_T)E'_T/\sum P(E'_T)$, of 61 and 69 kJ mol^{-1}, at low and high E_c, respectively, and their high energy tail extends up to 210 kJ mol^{-1}. For the $P(E'_T)$ at high E_c (solid line) the error bars of its determination are also indicated with shading.

To address the questions (1) which C_2HN isomer is obtained from the $N(^2D) + C_2H_2$ reaction and (2) which is the bound intermediate formed during the reaction, we combine the experimental observation to ab initio calculations.

Electronic Structure Calculations. The lowest doublet potential energy surface (PES) has been considered, but the transition state structure and the barrier height of the ground-state reaction $N(^4S) + C_2H_2(^1\Sigma_g^+)$ have been computed as well

(31) Miller, W. B.; Safron, S. A.; Herschbach, D. R. *Faraday Discuss.* **1967**, *44*, 108, 291.

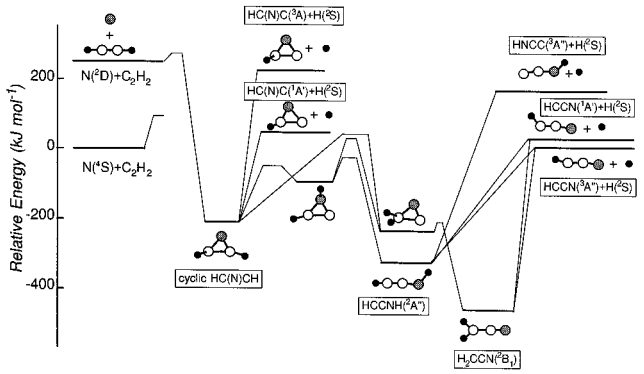

Figure 6. Schematic energy level and correlation diagram for the reaction $N(^2D) + C_2H_2(^1\Sigma_g^+)$ based on molecular orbital electronic structure calculations.

(a barrier of 86 kJ mol^{-1} is obtained, which explains the extremely low reactivity of $N(^4S)$). The schematic energy level diagram (Figure 6) shows the possible reaction pathways on the lowest doublet PES leading to N/H exchange. Our calculations indicate that in the initial step $N(^2D)$ adds to the π-system of the C_2H_2 molecule[32] forming cyclic HC(N)CH, a three-member ring radical situated 411 kJ mol^{-1} below the reactants. While the C_{2v} approach is found to be energetically the most favorable, a large barrier was found for the insertion of $N(^2D)$ into the C−H bond or for direct H-abstraction. The HC(N)CH radical can either decompose directly to cyclic HC(N)C(^{1}A′,^{3}A) + $H(^2S)$ or isomerize (via H-migration and ring opening) to HCCNH(^{2}A″) and/or $H_2CCN(^2B_1)$ (cyanomethyl). Cyanomethyl is found to be the global minimum on the doublet PES and is bound by 652 kJ mol^{-1} with respect to the reactants. Its enthalpy of formation is in agreement with previously reported values.[33] The propargylene-like radical HCCNH(^{2}A″) lies 134 kJ mol^{-1} above $H_2CCN(^2B_1)$. Both HCCNH(^{2}A″) and $H_2CCN(^2B_1)$ can dissociate into the lowest product channel, HCCN(^{3}A″) + $H(^2S)$ (the calculated reaction exoergicity is 211.3 kJ mol^{-1}). It should be noted that stabilization of the initial radical adduct is not expected under the single-collision conditions of the experiment. Formation of HCCN(^{1}A′) + $H(^2S)$, which lies about 50 kJ mol^{-1} above the ground-state HCCN(^{3}A″), is also possible. Formation of the third isomer HNCC(^{3}A″) from the decomposition of HCCNH(^{2}A″) is energetically less favored.

Discussion

The energy level and correlation diagram of Figure 6 forms the basis of the discussion. The CM angular and translational energy distributions shown in Figure 4 allow an evaluation of the dynamical influence of the potential energy surface and of kinematic constraints.

The energy cutoff of the $P(E'_T)$ distribution (Figure 4a) defines the maximum energy available to products; specifically, for the high E_c case the arrows indicate the total available energy for formation of the various possible isomer products from $N(^2D) + C_2H_2$. It it is clear that the $P(E'_T)$ is consistent with both HCCN(^{3}A″,^{1}A′) + $H(^2S)$ ($\Delta H°_0 = -211.7$ and -163 kJ mol^{-1}, respectively)[34,35] and HC(N)C(^{1}A′) + $H(^2S)$ ($\Delta H°_0 = -182$ kJ mol^{-1}) channels, while HNCC(^{3}A″) + $H(^2S)$ ($\Delta H°_0 = -71.5$ kJ mol^{-1}) must be minor. The extent of the $P(E'_T)$ distributions clearly shows that the C_2HN product is coming from the $N(^2D)$ reaction and not, for instance, from $N(^4S) + C_2H_2$ for which the total available energy would be 230.5 kJ mol^{-1} lower than that for $N(^2D) + C_2H_2$.

A high degree of product rotational excitation is expected, due the specific mass combination of this reaction, on the basis of angular momentum conservation arguments[30] and is witnessed by the lack of polarization of the CM angular distribution $T(\theta)$ (Figure 4b). The $T(\theta)$ is isotropic at $E_c = 13.0$ kJ mol^{-1} and becomes preferentially peaked in the forward (with respect to the N atom) direction ($\theta = 0°$) as the collision energy is increased to 39.7 kJ mol^{-1}. This behavior is typical of the occurrence, at low E_c, of a long-lived complex intermediate, i.e., a complex whose lifetime τ is considerably longer than its rotational period τ_r, and at high E_c of an osculating complex, i.e., a complex whose τ is comparable to τ_r. A ratio τ/τ_r of 1.16 is derived from the asymmetry of the $T(\theta)$ distribution within the osculating model[31] for chemical reaction by means of the relation $T(\theta{=}180°)/T(\theta{=}0°) = \exp(2\tau/\tau_r)$. The shift from a backward/forward symmetric to a forward biased CM angular distribution with increasing E_c is well visible in the contour-map product flux representation of Figure 5.

From the potential energy well depth of all C_2H_2N isomers relative to reactants and products (Figure 6), $H_2CCN(^2B_1)$ is bound with respect to products by 440.6 kJ mol^{-1}, while HCCNH(^{2}A″) is bound by 306.7 kJ mol^{-1} and cyclic HCCNH by only 199.6 kJ mol^{-1}. RRKM calculations for a total energy corresponding to $E_c = 39.7$ kJ mol^{-1} give lifetimes, τ, of about 7, 3, and 0.5 ps, respectively. Using the rotational periods, τ_r, calculated from the ab initio structures ($\tau_r = 0.93$, 0.90, and 0.57 ps for H_2CCN, HCCNH, and cyclic-HCCNH, respectively), we conclude that cyclic-HCCNH and HCCNH(^{2}A″) should be the intermediates which give a ratio τ/τ_r (0.9 and 3.3, respectively) closer to the experimental τ/τ_r value of 1.16 (H_2CCN gives $\tau/\tau_r = 7.5$, a considerably too large value). The shape of the angular and translational energy distributions points to the same intermediates. Decomposition of the HCCNH(^{2}A″) complex through a bent transition state (the HNC angle in HCCNH is about 113°) is characterized by a strong torque exerted when the H-atom departs following N−H bond cleavage, leaving a rapidly rotating HCCN moiety; in addition, contraction of the C−N bond and extension of the C−C and C−H bonds in going from HCCNH(^{2}A″) to HCCN(^{3}A″,^{1}A′) is expected to lead to considerable stretching excitation. Indeed, considerable vibrational excitation is expected from the modest (∼30%) fraction of the total available energy released in product translation. Our ab initio results show that the lowest energy path is that leading to HCCNH(^{2}A″), despite the higher stability of $H_2CCN(^2B_1)$ (Figure 6). On the contrary, dissociation of the H_2CCN complex would lead to a HCCN product with excited rotations around its internuclear axis, but due to the vanishing moment of inertia this rotation is not energetically accessible, and this pathway cannot account for rotational excitation in HCCN. Although the scattering data cannot fully discriminate between formation of the nearly linear HCCN and cyclic-HCCN, we note that a minor geometrical rearrangement accompanies the decomposition of the considerably short-lived cyclic HCCHN intermediate to cyclic-HCCN(^{1}A′) + $H(^2S)$. Indeed, our RRKM calculations on the decomposition of the HCCNH(^{2}A″) and cyclic-HCCNH intermediates indicate that HCCN + H and cyclic-HCCN + H are the main pathways, with branching ratios of (HCCN + H): (cyclic-HCCN + H) estimated to be 86:14 and 77:28 at E_c=13.0 and 39.7 kJ mol^{-1}, respectively. In conclusion, the above

(32) The calculated barrier height is 12 kJ mol^{-1}, but observation of product at $E_c = 13.0$ kJ mol^{-1} indicates that the calculated barrier is too high, corroborating the experimental activation energy of 2 kJ mol^{-1}.[11]

(33) Holmes, J. L.; Mayer, P. M. *J. Phys. Chem.* **1995**, *99*, 1366−1370.
(34) Francisco, J. S. *Chem. Phys. Lett.* **1994**, *230*, 372−376.
(35) Goldberg, N.; Fiedler, A.; Schwarz, H. *J. Phys. Chem.* **1995**, *99*, 15327−15334.

arguments suggest the nearly linear[36] HCCN to be the main product of the $N(^2D) + C_2H_2$ reaction at these low collision energies.[37]

Comparison with Related Systems

It is useful to compare the dynamics of the $N(^2D) + C_2H_2$ reaction with those of the related reactions of acetylene with ground-state oxygen, $O(^3P)$, and carbon, $C(^3P)$, atoms. (We recall that the reaction of ground-state nitrogen atoms, $N(^4S)$, with C_2H_2, although nearly thermoneutral, has a large energy barrier (see Figure 6) and hence does not occur at low collision energies).

$C(^3P) + C_2H_2$. The $C(^3P) + C_2H_2$ system most closely resembles the $N(^2D) + C_2H_2$ system from the point of view of the structure and energetics of the possible intermediates and products (see Figure 7a,b). The dynamics of the reaction of $C(^3P)$ with acetylene was recently elucidated by Kaiser et al.[38a] in combined crossed beam and ab initio studies.[38b] The product CM angular distribution was found to be forward peaked (with respect to the C atom direction) at low E_c and backward−forward symmetric at high E_c. It was concluded[38a] that the reaction proceeds via two microchannels initiated by addition of $C(^3P)$ to one acetylenic carbon to form *s-trans*-propenedylidene. Propenylidene undergoes [2,3]-H-migration to propargylene, followed by C−H bond cleavage via a symmetric exit transition state to linear C_3H and H, characterized by a backward−forward symmetric angular distribution. Propenylidene may also isomerize to triplet cyclopropenylidene and direct stripping dynamics via this cyclic intermediate contributes to the forward scattered second microchannel to form cyclic C_3H and H; this direct, forward-peaked contribution is quenched with rising collision energy. In the case of the $N(^2D)$ reaction, the cyclic HC(N)CH and linear HCCNH intermediates are the corresponding moieties of cyclic propenylidene, HC(C)CH, and propargylene, HCCCH. However, contrary to the $C(^3P)$ reaction, a forward scattered product angular distribution corresponding to direct stripping dynamics to form cyclic HCCN is not observed at low E_c. Whatever linear or cyclic HCCN is formed, in the case of the $N(^2D)$ reaction we observe the formation of a long-lived complex at low E_c; the lifetime of this complex decreases with increasing E_c and the complex starts to osculate giving a preferentially forward scattered angular distribution. Clearly, the different electronic structure of $N(^2D)$ with respect to $C(^3P)$ and the somewhat different energetics of the corresponding reactions with C_2H_2 should be responsible for the differences in dynamics observed.

$O(^3P) + C_2H_2$. The dynamics of the reaction of $O(^3P)$ with acetylene were elucidated by Schmoltner et al. in crossed beam studies.[39] The schematic energy diagram is shown in Figure 7 comparatively to that of $N(^2D) + C_2H_2$ and $C(^3P) + C_2H_2$. From

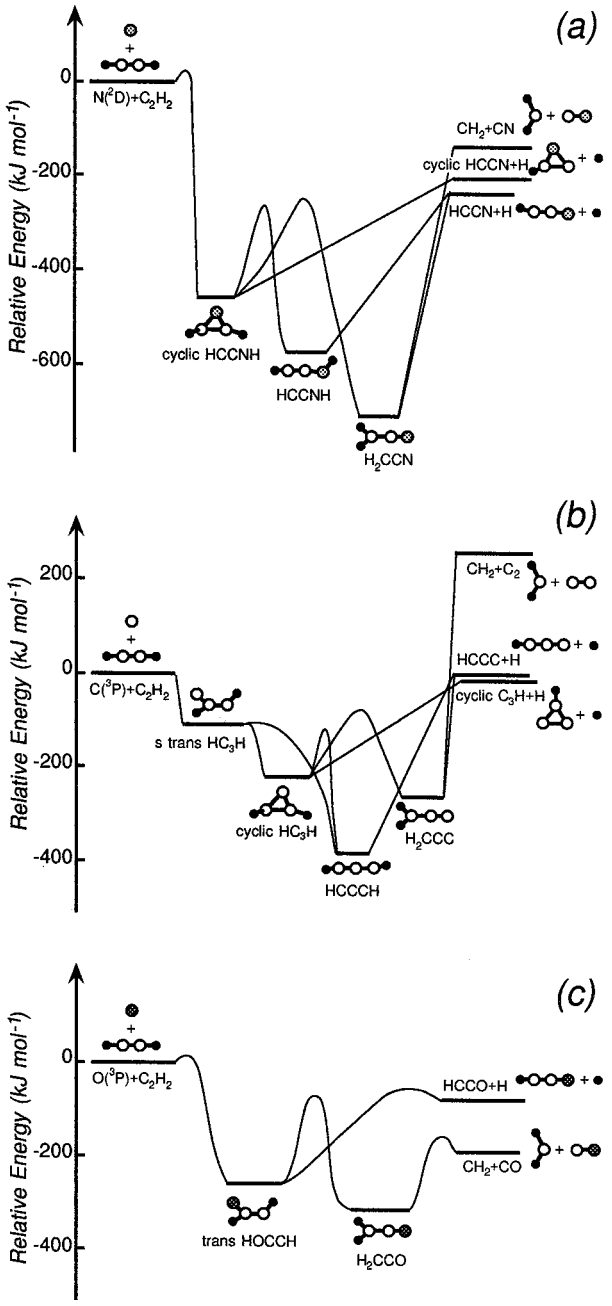

Figure 7. Schematic energy level and correlation diagrams for $N(^2D) + C_2H_2$ (a), $C(^3P) + C_2H_2$ (b) (adapted from ref 38a,b), and $O(^3P) + C_2H_2$ (c) (adapted from ref 39).

product angular and velocity distributions of the reaction products, it was found that the reaction proceeds via two pathways. Initial attack of the electrophilic oxygen atom to a π-orbital of one acetylenic carbon forms a long-lived *s-trans*-HCCOH on the triplet surface. This complex either fragments to the ketenyl radical HCCO and H ($\Delta H°_0 \sim -80$ kJ mol^{-1}) or undergoes [1,2]-H-migration to triplet ketene (H_2CCO) prior to decomposing into $CH_2 + CO$ ($\Delta H°_0 \sim -196$ kJ mol^{-1}). At $E_c \sim 25$ kJ mol^{-1} the branching ratio ($CH_2 + CO$):(HCCO + H) was estimated[39] to be 1.4 ± 0.5. The C−C bond cleavage channel in the $N(^2D)$ and $C(^3P)$ reactions would lead to the $CH_2 + CN$ and $CH_2 + C_2$ product channels, which are weakly exoergic ($\Delta H°_0 \sim -50$ kJ mol^{-1}) and strongly endoergic ($\Delta H°_0 \sim 257$ kJ mol^{-1}), respectively, because of the much smaller stability of the CN and C_2 radicals with respect to the CO molecule. Unfortunately, the $CH_2 + CN$ channel could not be investigated in the present study because the CN mass is

(36) The HCCN radical has received extensive experimental and theoretical attention about its structure characterization. See: (a) Aoki, K.; Ikuta, S.; Nomura, O. *J. Chem. Phys.* **1993**, *99*, 3809−3814. (b) McCarthy, M. C.; Gottlieb, C. A.; Cooksy, A. L.; Thaddeus, P. *J. Chem. Phys.* **1995**, *103*, 7779−7787. (c) Sun, F.; Kosterev, A.; Scott, G.; Litosh, V.; Curl, R. F. *J. Chem. Phys. A* **1998**, *109*, 8851−8856 and references therein.

(37) The present results do not allow us to ascertain if electronically excited $HCCN(^1A')$ is formed, since the singlet−triplet energy separation is only of the order of 50 kJ mol^{-1}. It is noteworthy, however, that the high-energy cutoff of our $P(E)$ is about 50 kJ mol^{-1} lower than the maximum total available energy corresponding to $HCCN(^3A'')$; so, singlet HCCN may well be formed.

(38) (a) Kaiser R. I.; Ochsenfeld, C.; Head-Gordon, M.; Lee, Y. T.; Suits, A. G. *J. Chem. Phys.* **1997**, *106*, 1729−1741. (b) Guadagnini, R.; Schatz, G. C.; Walch, S. P. *J. Phys. Chem. A* **1998**, *102*, 5857−5866.

(39) Schmoltner, A. M.; Chu, P. M.; Lee, Y. T. *J. Chem. Phys.* **1989**, *91*, 5365−5373.

identical with that of the C_2H_2 reagent; however, our RRKM calculations on the decomposition of the H_2CCN intermediate give a negligibly small branching ratio ($CH_2 + CN$):(HCCN + H). Regarding the initial cyclic adduct in the case of the oxygen reaction, formation of a cyclic triplet oxirene, HC(O)CH, complex is expected to involve a significant potential barrier resulting from electrostatic interaction of the doubly occupied p-orbital of oxygen with the closed shell acetylene molecule. The p-orbital is empty and partially occupied in the case of $C(^3P)$ and $N(^2D)$, respectively, and the electrostatic interaction is eliminated and reduced, respectively, leading to no reaction barrier in the case of the carbon atom and to a small barrier ($\sim$2 kJ mol^{-1}) for the excited N atom reaction.

Conclusions

The present crossed molecular beam results, together with the electronic structure and RRKM calculations, show that the reaction of $N(^2D)$ with acetylene is governed by an initial attack of the N atom to the π electron density of the C_2H_2 molecule to form a C_2H_2N collision complex, which decomposes in a time comparable to its rotational period into HCCN + H. From the extent of the product recoil energy, we derive that the cyanomethylene radical product has a considerable degree of internal excitation (about 70%).

Since HCCN is the main reaction product and is formed with a large cross section (the rate constant at 300 K[11] is 6.7 larger than requested in Yung's model[12a]), the reaction $N(^2D) + C_2H_2$ ($^1\Sigma_g^+$) can now be suggested to be the likely first step in the formation of nitriles in the upper atmosphere of Titan and must be included in chemical reaction networks modeling its atmosphere. Experiments currently under way in our laboratory show that reactions of $N(^2D)$ with other hydrocarbons, such as ethylene, may well be the source of carbon−nitrogen containing species, as acetonitrile (CH_3CN), observed in these extraterrestrial environments.[40] Finally, laboratory studies such as this are expected to contribute significantly to understanding data from the Cassini probe, a spacecraft with the scope of analyzing Titan's atmosphere within the CASSINI-HUYGENS mission.[41a−c]

From a more general point of view, the possibility of studying the reactive scattering of atomic nitrogen in CMB experiments has become reality owing to the novel capability of generating intense supersonic beams of nitrogen atoms. Other experiments are currently under way on $N(^2D)$ reactions with both organic and inorganic molecules. The aim is to gain an insight on the chemistry of this peculiar atomic species which has already revealed a rich complexity in its chemical behavior giving rise to addition, insertion, and abstraction reactions.

Acknowledgment. This work was supported by the Italian "Ministero Università e Ricerca Scientifica" (MURST- COFIN) and "Consiglio Nazionale delle Ricerche" (CNR) and the EEC Commission through the TMR program (contract No. FMRX-CT97-0132).

JA993448C

(40) Bézard, B.; Marten, A.; Paubert, G. *Bull. Am. Astron. Soc.* **1993**, *25*, 1100.

(41) (a) T. Owen, personal communication. (b) Taylor, F. W.; Coustenis, A. *Planet. Space Sci.* **1998**, *46*, 1085−1097. (c) See also: *Plane. Space Sci.* **1998**, *46*, No. 9/10 (Special issue on The Cassini/Huygens Mission to Titan and the Saturnian System, Edited by Cerroni, P., Coradini, A., Coustenis, A., Taylor, F.).